

Physics-Informed Artificial Neural Network-Based Estimation of Dielectric Properties for Resonant Method

Nur Sofia Idayu Didik Aprianto¹, Syamimi Mardiah Shahrarum¹, Nurfarhana Mustafa¹, Ahmad Afif Mohd Faudzi¹, Ahmad Syahiman Mohd Shah¹, Toshihide Kitazawa² and Mohamad Shaiful Abdul Karim^{1,*}

¹Faculty of Electrical and Electronics Engineering Technology, Universiti Malaysia Pahang Al-Sultan Abdullah, 26600 Pekan, Pahang, Malaysia

²Ritsumeikan University, 525-8577 Shiga, Japan

*Corresponding author: mshaiful@umpsa.edu.my

Submitted 21 September 2025; Revised 27 April 2026; Accepted 07 May 2026; Available online 14 May 2026.

Copyright © 2026 The Authors.

Abstract: Accurate determination of dielectric properties, particularly relative permittivity (ϵ_r) and loss tangent ($\tan \delta$), is essential in microwave material characterization. This paper proposes an artificial neural network (ANN)-based approach that leverages resonant features of a rectangular cavity resonator to estimate dielectric properties. Full-wave electromagnetic simulations in Computer Simulation Technology Studio Suite were performed over the X-band frequency range (8–12 GHz), covering a wide set of low-loss dielectric samples with permittivity between 1 and 10 and loss tangent values from 0.001 to 0.2. Transmission responses were generated, from which resonant frequency and quality factor (Q) were extracted as input features for a two-layer ANN implemented in MATLAB. The model achieved excellent predictive accuracy, with coefficient of determination values exceeding 0.999 and mean percentage errors below 0.2% for both ϵ_r and $\tan \delta$. Results demonstrate that resonant frequency is highly sensitive to permittivity variations, while Q-factor effectively captures dielectric losses. The proposed framework was further validated using a Teflon sample in the X-band, where the ANN predicted a relative permittivity of 2.01 and a loss tangent of 0.0014, in close agreement with literature values. These results highlight the potential of the proposed ANN framework for efficient and non-destructive dielectric property estimation.

Keywords: Artificial Neural Network; Dielectric characterization; Microwave resonator; Quality factor; Permittivity.

1. INTRODUCTION

Microwave engineering, a branch of electrical engineering, is widely applied in communications, radar, sensing, and material testing [1-3]. Among these, dielectric characterization is especially critical because relative permittivity (ϵ_r) and loss tangent ($\tan \delta$) govern how materials interact with electromagnetic fields, directly impacting the design and performance of antennas, resonators, and microwave circuits [4-6]. Cavity resonators are often considered the gold standard for dielectric measurement due to their high sensitivity [7-9]. In such structures, the resonant frequency (f_r) is strongly correlated with permittivity, while the quality factor (Q) reflects dielectric losses, making them established and reliable features for material property extraction [10]. Classical workflows typically require sweeping the full transmission response, identifying the resonance, and then applying electromagnetic (EM) simulations or calibrated inversion formulas to extract material properties. While effective, this process can be computationally heavy and repetitive when characterizing multiple materials, since each new dataset often requires fitting or consulting calibration curves.

Conventional approaches to dielectric extraction also face limitations. Analytical methods such as the Nicolson–Ross–Weir (NRW) technique rely on closed-form equations derived from S-parameters, but these are prone to numerical instability and reduced accuracy for low-loss dielectrics [11,12]. Numerical approaches based on full-wave solvers, including Finite Element Method (FEM), Method of Moments (MoM), and Finite-Difference Time-Domain (FDTD), provide higher fidelity but require significant computational effort. More recently, machine learning (ML) techniques have been introduced, with studies applying regression models and artificial neural networks (ANNs) directly to S-parameters. For example, Bonello *et al.* demonstrated the use of ANN models to estimate complex permittivity of biological tissues from microwave sensing measurements, showing that neural networks can approximate nonlinear electromagnetic relationships between measured signals and dielectric parameters [13]. Similarly, Tan *et al.* developed a deep learning assisted measurement system for dielectric characterization at microwave frequencies, where neural networks were trained using large datasets of electromagnetic responses to estimate material properties [14]. While these studies highlight the potential of ML techniques for dielectric characterization, they typically rely on high-dimensional electromagnetic inputs, typically derived from full S-parameter spectra, reflection coefficients, or broadband electromagnetic responses [4,13] as input features. Such approaches

increase data dimensionality and computational requirements, and often reduce interpretability since the learned relationships are purely data-driven rather than directly linked to physically meaningful resonant descriptors.

The gap lies in the absence of feature-compressed, physics-informed ML models that leverage the resonant characteristics of cavity resonators. Instead of relying on the full S-parameter spectrum, f_r and Q can serve as practical descriptors of a material's electromagnetic behaviour. Recent research on microwave sensing systems indicates that many machine-learning-based dielectric characterization approaches rely on planar resonators [15,16], free-space measurement setup [17], or broadband microwave sensor [18], where the entire transmission or reflection spectrum is used as the input for regression or classification models. While these approaches have demonstrated promising predictive performance, they generally utilize high-dimensional electromagnetic responses as input features. In contrast, resonant cavity systems provide physically interpretable parameters such as f_r and Q that directly relate to dielectric permittivity and loss.

In this work, ANN is positioned as a supporting tool to the resonant method. Using ideal simulated data, the ANN demonstrates that these two physics-meaningful features are sufficient to approximate both ϵ_r and $\tan \delta$ across a controlled parameter space. Once trained, the ANN provides near-instant predictions, thereby reducing dependence on repeated EM inversions. In this sense, the ANN streamlines the resonant method workflow while preserving its physical interpretability. While ML has been applied to microwave-based material characterization in different forms [13,14,19], the specific use of rectangular cavity resonator waveguides as inputs to ML models remains underexplored.

To address this, the present work proposes an ANN-based framework that predicts ϵ_r and $\tan \delta$ from f_r and Q , extracted from a rectangular cavity resonator operating across the X-band (8–12 GHz). The model incorporates log-scaling for $\tan \delta$ to improve stability in the low-loss regime and is evaluated on dielectric samples with ϵ_r ranging from 1–10 and $\tan \delta$ between 0.001–0.2. The main contributions of this work can be summarized as follows:

- Physics-informed ANN framework for dielectric characterization. This work proposes an ANN based approach that predicts the dielectric properties of materials using resonant characteristics extracted from a rectangular cavity resonator. Unlike conventional machine learning approaches that rely on full S-parameter spectra, the proposed model utilizes physically meaningful resonant descriptors.
- Feature-compressed representation using resonant parameters. The study demonstrates that two compact resonant features, namely the f_r and Q , are sufficient to approximate both ϵ_r and $\tan \delta$. This significantly reduces input dimensionality while preserving the essential electromagnetic information required for dielectric characterization.
- Improved stability for low-loss dielectric prediction. A logarithmic scaling strategy is introduced for the $\tan \delta$ during ANN training to enhance prediction stability in the low-loss regime, where $\tan \delta$ values are very small and difficult to model using conventional regression techniques. This allows the proposed model to reliably estimate dielectric loss across a wide range of materials.

2. METHODOLOGY

2.1 Selection of Resonator Model

The choice of resonator model is critical for achieving accurate results in dielectric characterization. Resonators provide valuable insights into the interaction between electromagnetic waves and materials, enabling the extraction of parameters such as ϵ_r and $\tan \delta$. An optimal resonator design improves measurement accuracy by minimizing errors such as energy losses.

Resonator geometries vary in terms of compatibility, complexity, and application. Cylindrical and rectangular cavities are commonly used, each offering specific advantages. Circular cylindrical cavities are often favoured for their high accuracy [16,17] and compatibility with soft materials. However, this method requires high-precision machining, and even small air gaps between the sample and cavity wall can significantly reduce accuracy [21]. Furthermore, input and output ports are often neglected in electromagnetic analysis, limiting their applicability to lossy materials where energy transfer effects are significant [22].

In this study, a rectangular cavity resonator is employed due to its suitability for dielectric testing. Compared to cylindrical cavities, it reduces the machining complexity since block- or bar-shaped samples can be inserted more easily. However, precise preparation is still required to minimize air gaps and ensure dimensional accuracy, as these remain critical factors for reliable dielectric property extraction. The design reduces the influence of air gaps, provides strong field confinement, and can accommodate samples with arbitrary cross-sectional geometries [23]. Moreover, the resonator had been fabricated and validated in prior work [23] making it a practical and time-efficient choice. This allowed the research to focus on the primary objective: dielectric property estimation using ANN.

2.2 Resonator Design and Simulation

The study begins by formulating the microwave resonator model using full-wave electromagnetic simulations in Computer Simulation Technology (CST) Studio Suite. The simulated dielectric samples cover a range of ϵ_r from 1 to 10 and $\tan \delta$ from 0.001 to 0.2, ensuring applicability across both low-loss and moderately lossy materials. Each sample was modelled with a cross-sectional size of $10 \times 10 \text{ mm}^2$ and a height equal to the waveguide's height dimension, t , (10.16 mm), corresponding to the X-band WR-90 waveguide, to ensure consistent interaction with the electromagnetic fields.

The rectangular cavity resonator was designed to achieve a target f_r of approximately 8.484 GHz, operating within the 8–12 GHz frequency band. The f_r of 8.484 GHz was selected in line with prior studies where a rectangular cavity coupled with waveguides demonstrated stable resonance at the TE₃₀₄ mode around 8.48 GHz. Abdul Karim *et al.* [23] confirmed through hybrid EM analysis and experimental validation that this frequency provides reliable scattering characteristics for material characterization, thereby justifying its adoption in this work. Its design emphasized a high Q -factor to improve sensitivity and minimize measurement uncertainties during dielectric characterization. For simulation purposes, the cavity was modelled in

CST Studio Suite with Perfect Electric Conductor (PEC) boundaries to represent an idealized, lossless structure. This ensured that the initial analysis focused on dielectric material effects, with future refinements to include practical metallic boundaries for experimental validation.

The design parameters of the rectangular cavity resonator are summarized in Table 1. These dimensions were adopted from prior work [23], where the design demonstrated high efficiency and reliability for dielectric measurements. The rectangular cavity resonator model with its key dimensions is shown in Figure 1. The material under test (MUT) was modelled as a block with dimensions $L_m = 10$ mm and $W_m = 10$ mm. The MUT was placed at the centre of the cavity.

2.3 Resonant Frequency and Q -factor for Accuracy Determination

The f_r and Q -factor are essential parameters for evaluating the accuracy of permittivity estimation. The f_r is influenced by the real part of complex relative permittivity, ϵ_r' , which determines how the material stores electric energy. In a cavity resonator, a higher ϵ_r' slows wave propagation, thereby lowering f_r , [24]. Thus, shifts in f_r can be directly related to variations in relative permittivity (ϵ_r') [25].

The Q -factor reflects the dielectric losses, governed by the imaginary part of complex relative permittivity (ϵ_r''), which represents energy dissipation as heat. Materials with higher ϵ_r'' broaden the resonance peak, resulting in lower Q -factors, while low-loss materials yield sharper peaks and higher Q -factors. The Q -factor can be quantitatively determined from the -3 dB bandwidth of the resonance curve, as illustrated in Figure 2. It is defined as in Equation (1) where the f_r is the resonant frequency at the peak of the resonance curve, and $\Delta f = f_2 - f_1$ is the bandwidth between the two frequencies (f_1 and f_2) at which the amplitude decreases by 3 dB from the peak. The narrower the bandwidth, the higher the Q -factor, indicating lower dielectric losses, while broader bandwidths correspond to higher material losses.

$$Q = \frac{f_r}{\Delta f} \tag{1}$$

Therefore, by accurately extracting both f_r and Q -factor from S-parameter measurements, one can reliably determine the complex permittivity of the material. In the context of this research, these two parameters serve as essential evaluation metrics for verifying the accuracy of dielectric property estimation using the proposed ANN approach.

2.4 ANN Architecture Design

In this work, a supervised ANN model was developed in MATLAB to predict dielectric properties using ML. The goal was to estimate ϵ_r and $\tan \delta$ directly from the extracted f_r and Q values of S_{21} responses. This section details the ANN implementation in three stages: architecture design, training methodology, and validation of the trained model.

Figure 3 illustrates the overall workflow of the proposed machine learning-based material characterization system. The process begins with the electromagnetic simulation of a rectangular waveguide resonator using CST Studio Suite. The simulated S-parameter response is analyzed to identify the f_r and the Q using the -3 dB bandwidth method. These two parameters form critical input features for the prediction model.

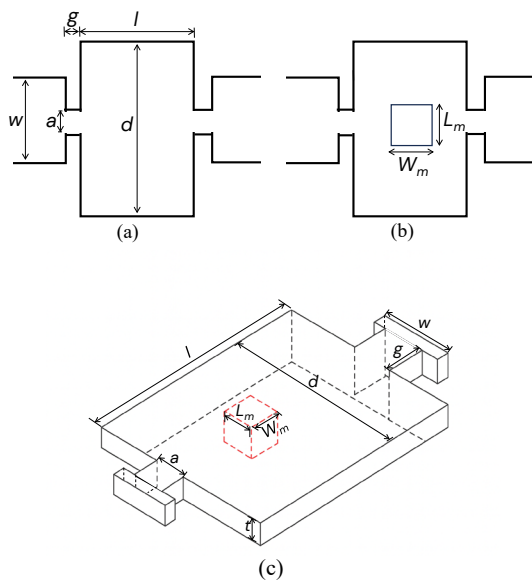


Figure 1. (a) Top view of the rectangular cavity resonator with connected waveguides; (b) Placement of the MUT inside the cavity resonator; (c) Three-dimensional isometric view.

Table 1. Design parameters of the rectangular cavity resonator.

Parameter	Value (mm)
Width of waveguide, w	22.860
Gap size of waveguide, a	2.480
Depth of cavity, d	68.569
Coupling gap, g	0.003
Length of cavity, l	111.330

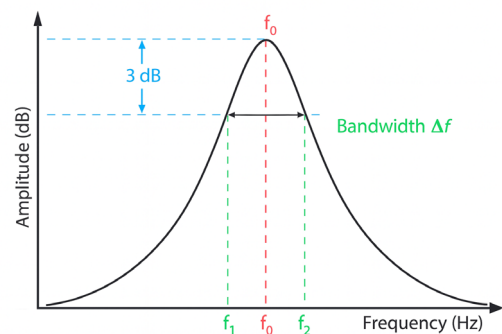


Figure 2. Q -factor calculation based on -3 dB bandwidth.

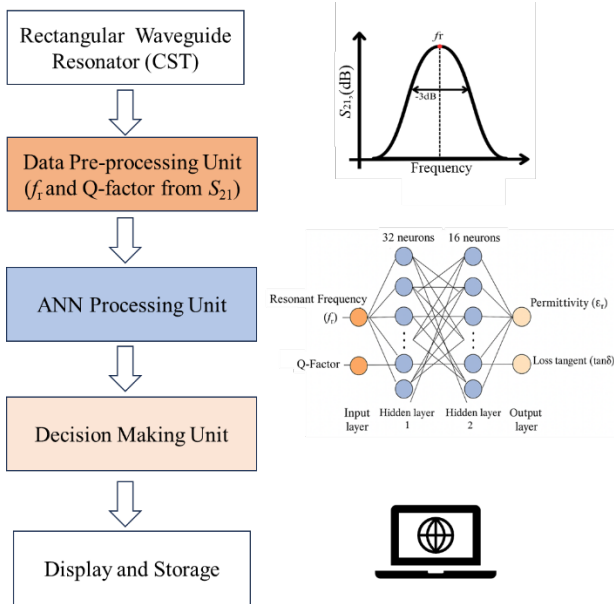


Figure 3. ANN-based dielectric prediction flow.

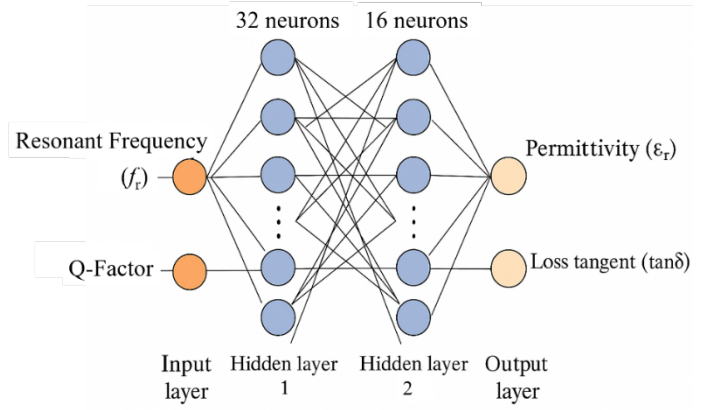


Figure 4. ANN model for dielectric properties prediction.

In the data pre-processing unit, f_r and Q are extracted from the S_{21} spectrum using curve-fitting techniques applied to either full-resolution or reduced-resolution data, depending on the sampling strategy employed. These inputs are then passed into an ANN, which is structured with two hidden layers comprising 32 and 16 neurons, respectively. The ANN maps the resonance features to dielectric material properties, specifically the ϵ_r and the $\tan \delta$, which are the final outputs of the model. A decision-making unit evaluates the ANN outputs, possibly applying thresholds or classification logic, if necessary. Finally, the system's outputs are directed to the display and storage unit, which may serve as an interface for real-time monitoring, result logging, or integration with other systems.

The ANN was constructed using MATLAB's *fitnet* function, configured as a two-layer feedforward network. The input layer accepts two features: f_r and Q -factor. The output layer produces two outputs corresponding to the real-valued ϵ_r and $\tan \delta$ of the material under test. The chosen architecture includes 32 neurons in the first hidden layer and 16 neurons in the second, both using the default *tansig* activation function. The selection of this structure was based on empirical testing and trade-offs between training performance and overfitting. Figure 4 illustrates the ANN architecture used in this study. In addition, log-scaling of the $\tan \delta$ was introduced during training. This transformation was particularly important for enhancing numerical stability in the low-loss regime, where $\tan \delta$ values are very small and conventional linear-scale training often leads to poor convergence or biased predictions.

2.4.1 Training of the ANN

The ANN was trained using the Levenberg–Marquardt backpropagation algorithm (*trainlm*), which is widely preferred for function approximation due to its fast convergence. For each level of sampling density, the ANN was trained independently to observe the impact of data reduction on prediction accuracy.

Training data were split into 70% training, 15% validation, and 15% testing subsets. Input features were normalized automatically by MATLAB's training function. The network was trained for up to 1000 epochs or until validation performance ceased to improve after six consecutive attempts (early stopping). During each iteration, the forward pass computes predicted values, and the error between predicted and true values is minimized using backpropagation.

2.4.2 Validation and Performance Evaluation

Model performance was evaluated using several standard statistical regression metrics to quantify prediction accuracy for both ϵ_r and $\tan \delta$. These include Mean Squared Error (MSE), Root Mean Square Error (RMSE), Mean Absolute Error (MAE), and the coefficient of determination (R^2). Each metric provides a different perspective on the quality of the ANN predictions compared to the ground truth values from CST simulations.

The MSE is defined as in Equation (2), where y_i is the true target value, \hat{y}_i is the predicted value by the ANN, and N is the total number of samples. This metric penalizes larger errors more severely due to the squared term. A high MSE indicates large deviation or may suggest overfitting or underfitting. The RMSE is derived as the square root of MSE as shown in Equation (3), RMSE has the advantage of being in the same units as the predicted variable, making it more interpretable. Unlike MSE, MAE as shown in Equation (4) is less sensitive to outliers and provides a more general sense of average error magnitude. Finally, the coefficient of determination (R^2) measures how well the model explains the variance in the data. It is expressed in Equation (5) where \bar{y} is the mean of the true target values. An R^2 value close to 1 indicates that the model captures most of the variance in the data, while a value near zero indicates poor predictive performance.

$$MSE = \frac{1}{N} \sum_{i=1}^N (y_i - \hat{y}_i)^2 \tag{2}$$

$$\text{RMSE} = \sqrt{\frac{1}{N} \sum_{i=1}^N (y_i - \hat{y}_i)^2} \quad (3)$$

$$\text{MAE} = \frac{1}{N} \sum_{i=1}^N |y_i - \hat{y}_i| \quad (4)$$

$$R^2 = 1 - \frac{\sum_{i=1}^N (y_i - \hat{y}_i)^2}{\sum_{i=1}^N (y_i - \bar{y})^2} \quad (5)$$

3. RESULT AND DISCUSSION

An ANN was developed to predict the dielectric properties, namely ϵ_r and $\tan \delta$, from the resonant response of a rectangular waveguide cavity resonator. Instead of using the full S_{21} spectrum as input, two resonant features, the f_r and Q -factor, were extracted from the S_{21} response and employed as compressed physical descriptors of the material’s electromagnetic behavior. These parameters act as practical substitutes, correlating resonator response to dielectric properties.

3.1 Model Training Performance

The ANN was implemented using the Levenberg–Marquardt backpropagation algorithm (*trainlm*) with a two-hidden-layer architecture comprising 32 and 16 neurons, respectively. The training process completed in 186 iterations, achieving the best validation performance with a MSE of 1.36×10^{-4} at epoch 180, as illustrated in Figure 5. The error curves for training, validation, and test datasets decreased simultaneously during the early epochs, indicating that the network quickly learned the fundamental relationship between cavity resonator features and dielectric properties. After approximately 50 epochs, the curves flattened, with the validation and test errors remaining closely aligned with the training error. This stability suggests that the ANN generalized well to unseen data without evidence of overfitting.

From a microwave engineering perspective, such convergence behavior is critical. Accurate prediction of ϵ_r and $\tan \delta$ requires capturing the sensitivity of the f_r to permittivity variations, as well as the dependence of the Q -factor on dielectric losses. The ANN’s stable training confirms that these nonlinear dependencies were successfully modelled. In practical terms, this ensures that the cavity resonator method, when combined with the trained ANN, can demonstrate potential to provide rapid and precise dielectric properties extraction across a wide range of materials, including low-loss dielectrics where small deviations in $\tan \delta$ strongly influence the Q -factor.

3.2 Prediction of Dielectric

Following successful training, the model was evaluated on its ability to predict both ϵ_r and $\tan \delta$. Figure 6(a) shows the predicted versus true values of relative permittivity, where the results align closely with the 1:1 line, confirming accurate prediction across the full permittivity range (1–10). In the cavity resonator method, the f_r is strongly related to the dielectric permittivity of the material under test, since changes in ϵ_r affect the stored electromagnetic energy and shift the resonance. The ANN results are consistent with this behavior, showing that the network was able to approximate the relationship between resonant features and permittivity values.

This outcome suggests that the proposed approach can provide a practical means of predicting permittivity without relying on the full frequency spectrum. While the agreement is strong, the model should still be interpreted as a supportive tool for cavity resonator analysis rather than a replacement for direct measurement. Within this scope, the ANN demonstrates reliable performance in capturing the trend of permittivity variation across the tested range, which is relevant for microwave engineering applications such as substrates and dielectric characterization. Figure 6(b) presents the comparison between predicted and true values of the $\tan \delta$ in the original scale. The ANN predictions follow the 1:1 line closely, indicating strong agreement with the true values across the tested range of 0.001–0.2.

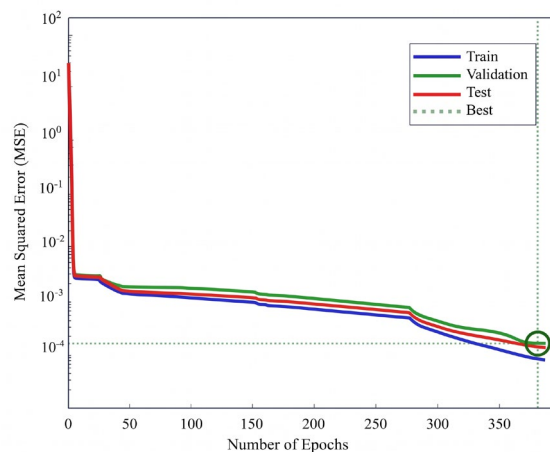


Figure 5. Training performance curve of the ANN model.

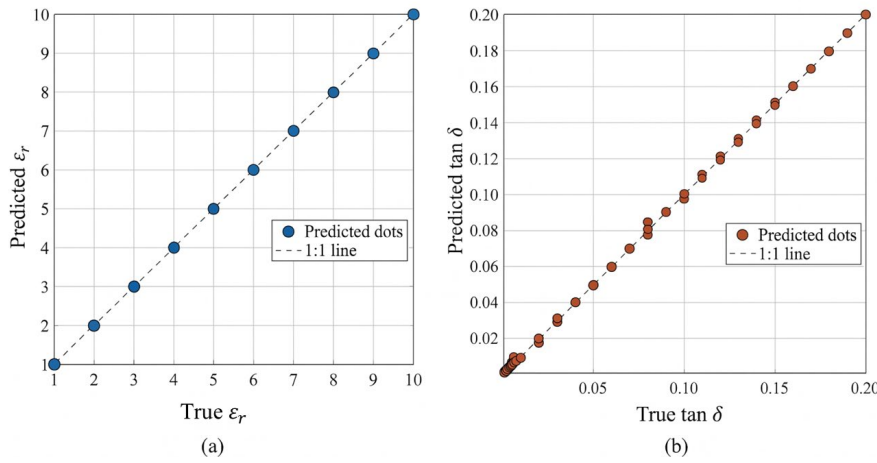


Figure 6. Comparison of predicted and true values of (a) relative permittivity (ϵ_r) and (b) loss tangent ($\tan \delta$) in the original scale.

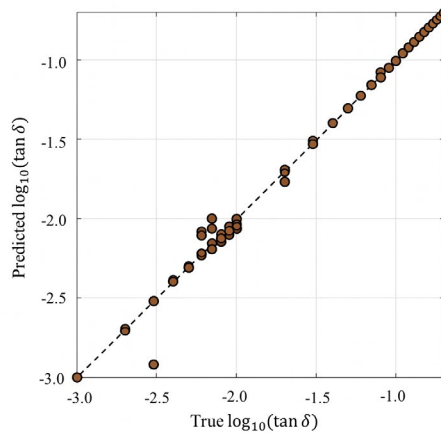


Figure 7. Predictions of loss tangent in the training space ($\log_{10}(\tan \delta)$).

In cavity resonator measurements, the Q -factor is particularly sensitive to dielectric losses, where even small variations in $\tan \delta$ can lead to noticeable changes in the resonator bandwidth. Capturing this sensitivity accurately is challenging, especially in the low-loss regime ($\tan \delta < 0.01$), where the signal differences are subtle. To address this, $\tan \delta$ was trained in logarithmic scale, which improved stability for very small values. This approach helped the ANN maintain predictive accuracy across both low-loss and higher-loss samples.

The close alignment between predicted and true $\tan \delta$ values suggests that the model effectively utilized the Q -factor information to approximate dielectric losses. While this does not replace direct cavity measurements, it shows that the ANN can serve as a reliable supporting tool for interpreting resonant responses, particularly where rapid evaluation of multiple samples is required.

Figure 7 shows the predicted versus true values of $\tan \delta$ in the logarithmic training space, $\log_{10}(\tan \delta)$. Most data points align closely with the 1:1 line, indicating that the ANN maintained stability when predicting across several orders of magnitude. This representation highlights the model’s behavior in the low-loss regime ($\tan \delta \approx 10^{-3}$), where regression tasks are typically more challenging due to the narrow resonance bandwidths associated with very high- Q cavities. While the predictions in the original scale (Figure 6(b)) show excellent agreement across the full range of $\tan \delta$, the logarithmic representation in Figure 7 provides additional insight into the low-loss region. In the normal scale, small differences at very low values of $\tan \delta$ appear visually negligible compared to higher-loss values. By contrast, the log-scale view expands this region and reveals that predictions below $\tan \delta < 0.01$ exhibit slightly greater scatter around the 1:1 line.

This observation is consistent with the cavity resonator method, where ultra-low-loss materials correspond to very high Q -factor. In such cases, the resonance bandwidth becomes extremely narrow, and even small numerical or experimental uncertainties can lead to noticeable variations in the extracted $\tan \delta$. The ANN predictions reflect this challenge, showing that while the model remains stable in the low-loss regime, it is naturally more sensitive in capturing losses associated with very high- Q resonances. Thus, the log-scale results confirm that the ANN performs reliably across the tested range, while highlighting the practical limitations of predicting ultra-low-loss values, a region where both computational models and measurement systems are inherently more demanding.

Taken together, the results in Figures 6 and 7 demonstrate that both key dielectric properties, ϵ_r and $\tan \delta$, can be reliably predicted from the compressed resonant features of the cavity resonator. By using only the f_r and Q -factor as inputs, the ANN captures the essential physical relationships between resonator response and material properties, without requiring the full frequency spectrum. This supports the feasibility of the proposed approach as a computationally efficient complement to conventional cavity resonator analysis.

3.3 Quantitative Evaluation

To further validate the predictive accuracy, the overall performance of the ANN was quantified using four standard statistical metrics: MSE, RMSE, MAE and R^2 . The results, summarized in Table 2, demonstrate excellent predictive capability for both ϵ_r and $\tan \delta$. For ϵ_r , the model achieved an MSE of 8.24×10^{-5} , RMSE of 0.0091, MAE of 0.0032, and $R^2=0.99999$, corresponding to a mean percentage error below 0.1%. These values indicate that the predicted permittivity deviates by less than 1% of a single permittivity unit, which is negligible relative to the tested range (1–10). For the $\tan \delta$, the model achieved an even lower MSE of 5.16×10^{-7} , RMSE of 0.00072, MAE of 0.00041, and $R^2=0.99988$, with mean percentage error below 0.2%. Such small errors confirm that the ANN successfully captured the strong nonlinear dependence between resonant features and dielectric loss, even in the low-loss regime where prediction is most challenging. These error levels are considerably lower than typical experimental uncertainties reported in cavity resonator measurements, which often range between 1–2% for permittivity and 5–10% for $\tan \delta$. Thus, the results establish that f_r and Q -factor are valid substitutes for precise prediction of dielectric properties.

3.4 Error Distribution Analysis

To further examine the reliability of the ANN predictions, the error distribution was analyzed through an error histogram with 20 bins, as shown in Figure 8. Most errors are highly concentrated around zero, with more than 500 instances falling within a very narrow error range between -0.002 and $+0.002$. Only a negligible number of samples deviate beyond this central cluster, and even those deviations remain within small absolute error values.

This tight clustering around zero error indicates that the ANN predictions for both ϵ_r and $\tan \delta$ are highly consistent with the true values. The absence of large outliers confirms that the model not only achieves strong average performance, as reflected in the MSE and R^2 metrics, but also maintains robustness across individual samples. Such an error distribution highlights the stability of the model and its suitability for precise dielectric property extraction from resonant features.

In summary, this baseline model trained on full-resolution data confirms that f_r and Q -factor serve as highly effective features for predicting dielectric properties via ML. The results serve as a reference point for evaluating performance degradation. Ultimately, this proves the feasibility of using a rectangular waveguide resonator combined with ANN for accurate, efficient, and non-destructive material characterization.

3.5 Experimental Validation

Experimental validation was carried out to evaluate the ability of the trained ANN model to predict the dielectric properties of materials using experimentally measured resonant parameters and then compared to the literature value. To verify the model, Teflon was used, as it is well known and widely used for microwave characterization verification because it meets the low-loss requirements of this study. The experimental measurements were conducted using a rectangular cavity resonator connected to a vector network analyzer (VNA) with Teflon sample placed at the center of the rectangular cavity resonator, as shown in Figure 9.

3.5.1 Experimental Evaluation of the ANN Model

In the representative measurement shown in Figures 10(a) and 10(b) and summarized in Table 3, inserting the Teflon sample into the cavity causes the resonant frequency to shift from 8.4824 GHz for the air-filled cavity to 8.4649 GHz for the loaded cavity, corresponding to a downshift of approximately 17.5 MHz. This behavior is expected because the resonant frequency depends on the effective permittivity within the cavity field region, and introducing a dielectric material with $\epsilon_r > 1$ reduces the resonant frequency [26]. The Q -factor also decreases slightly from 2492.5 to 2422.1 ($\approx 2.8\%$), reflecting the additional loss introduced by the dielectric sample [27]. The resonance remains narrow and well defined in both cases. Since the observed frequency shift (17.5 MHz) is much larger than the resonance peak width (≈ 3.49 MHz), the f_r and Q -factor can be clearly determined from a single measurement sweep.

Table 2. Performance metrics of the ANN for predicting ϵ_r and $\tan \delta$.

Performance Metric	ϵ_r	$\tan \delta$
MSE ($\times 10^{-5}$)	8.24	0.0516
RMSE	0.0091	0.00072
MAE	0.0032	0.00041
R^2	0.99999	0.99988
Mean % Error	< 0.1 %	< 0.2 %

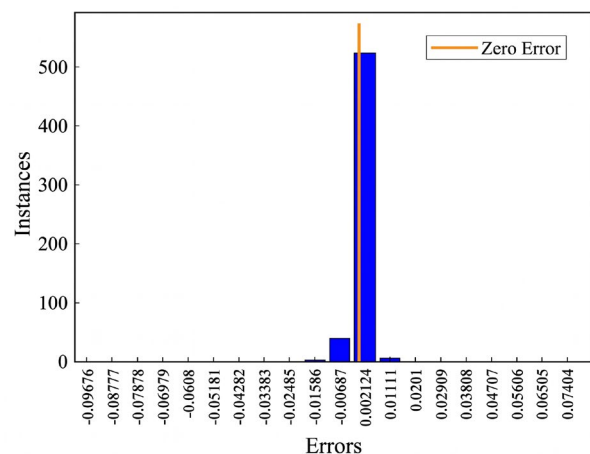


Figure 8. Error histogram of ANN predictions for relative permittivity (ϵ_r) and loss tangent ($\tan \delta$).

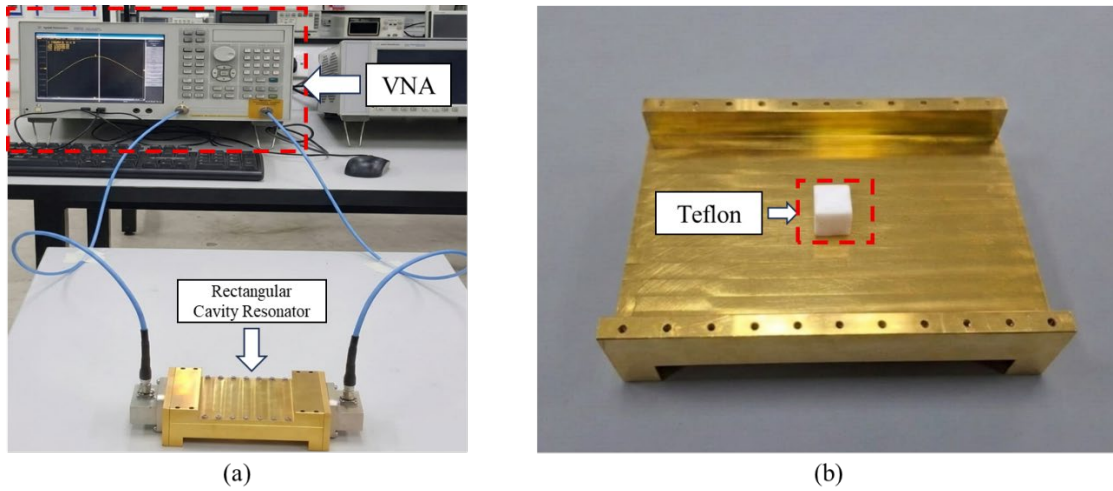


Figure 9. Experimental setup for dielectric measurement: (a) VNA connected to the rectangular cavity resonator (b) Teflon sample placed at the center of the cavity.

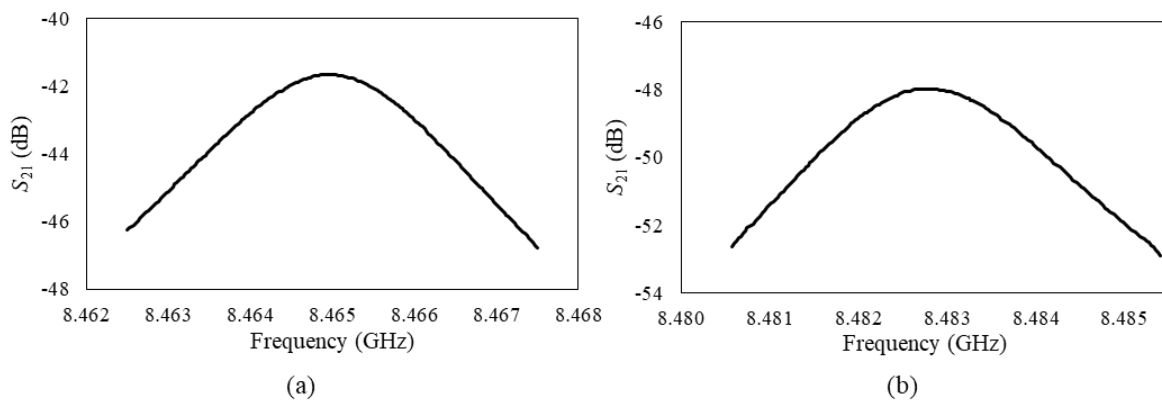


Figure 10. Measured S_{21} resonance of the cavity resonator under: (a) Teflon-loaded (b) air-filled conditions.

Table 3. Experimental measurements of Teflon and empty cavity.

Teflon		Air	
f_r (GHz)	Q -factor	f_r (GHz)	Q -factor
8.4649	2422.1	8.4824	2492.5

Table 4. Comparison of predicted results and literature standards.

Method	ϵ_r	$\tan \delta$
Literature value [28]	2.01	0.0015
Extracted using method in [23]	2.08	0.0011
Estimated by ANN	2.01	0.0014

Table 4 compares the dielectric parameters predicted by the proposed ANN model with values reported in previous studies. For Teflon in the X-band frequency range, the ANN-predicted values ($\epsilon_r = 2.01$, $\tan \delta = 0.0014$) show excellent agreement with literature data reported by Yakubu *et al.* [28] ($\epsilon_r = 2.01$, $\tan \delta = 0.0015$) and measurements obtained via the method in Abdul Karim *et al.* [23] ($\epsilon_r = 2.08$, $\tan \delta = 0.0011$). These results fall consistently within the typical range for Teflon, which is a well-characterized low-loss microwave material.

Minor variations between these values are expected. These discrepancies likely arise from differences in experimental conditions, sample preparation, or measurement procedures. However, the high degree of accuracy, particularly the near-exact match for permittivity, indicates that the ANN model effectively captures the complex relationship between resonant cavity features and material properties. While ϵ_r is often the primary driver for determining electromagnetic behavior in antenna design [29], the model’s ability to also estimate $\tan \delta$ is crucial for applications where dielectric losses are significant, such as microwave absorbers [30]. Ultimately, this comparison validates the use of machine learning as a supporting tool for dielectric characterization.

4. CONCLUSION

This work presented an artificial neural network (ANN)-based method for estimating dielectric properties using resonant responses of a rectangular cavity resonator. By utilizing f_r and Q -factor as compressed features, the ANN was able to predict ϵ_r and $\tan \delta$ with high accuracy. Across the X-band frequency range of 8–12 GHz, the model was trained and validated on dielectric samples spanning permittivity values between 1 and 10 and loss tangents from 0.001 to 0.2. The ANN achieved R^2

values above 0.999, with mean percentage errors below 0.1% for ε_r and below 0.2% for $\tan \delta$, demonstrating high reliability in identifying complex permittivity from resonant shifts. From a physical standpoint, the f_r reliably captured the relationship with permittivity, while the Q -factor reflected the sensitivity of the resonator to dielectric losses, particularly in low-loss materials. Training in logarithmic scale further improved prediction stability for very small $\tan \delta$ values, where regression models typically struggle due to high- Q resonances.

To conclude, the findings indicate that combining resonant feature extraction with ANN modelling can serve as a practical supporting tool for dielectric properties characterization. The proposed framework was validated using a Teflon sample, where the ANN predicted a $\varepsilon_r = 2.01$ and $\tan \delta = 0.0014$. These values show good agreement with literature values of approximately $\varepsilon_r = 2.01$ and 2.08 and $\tan \delta = 0.0015$ and 0.0011 reported for Teflon in the X-band frequency range. Minor differences between the predicted and reported values may arise from experimental factors such as sample positioning, measurement conditions, and cavity losses. The results demonstrate that combining resonant feature extraction with ANN modelling provides a practical approach for estimating dielectric properties. The agreement between the ANN predictions and experimental measurements confirms the capability of the proposed framework to capture the relationship between resonant parameters and material dielectric properties. This approach can therefore support dielectric characterization and assist in the design and analysis of resonant measurement systems.

ACKNOWLEDGMENT AND FUNDING

The authors would like to thank the Ministry of Higher Education for providing financial support under Fundamental Research Grant Scheme (FRGS-EC) No. FRGS-EC/1/2024/TK07/UMPSA/02/1 (University reference RDU243718) and Universiti Malaysia Pahang Al-Sultan Abdullah for laboratory facilities as well as additional financial support under Internal Research grant RDU240319 and PGRS230355.

DECLARATION OF CONFLICTING INTERESTS

The authors declare no potential conflicts of interest with respect to the research and publication of this article.

REFERENCES

- [1] C. Li, Z. Li, C. Zhang, N. Cheng, L. Guan and D. Wang, Achieving reliable and intelligent control-assisted transmission for satellite communications, *IEEE Conference on Computer Communications Workshops (INFOCOM WKSHPS)*, Vancouver, Canada, 2024, 1–6.
- [2] Y. Rahayu, B. Kurniawan and Y. P. Saputera, Narrow wall beamwidth slotted waveguide antenna for portable coastal radar communication, *Journal of Engineering Science and Technology*, 18, 2023, 60–70.
- [3] M. M. Alam, N. A. T. Yusof, Y. A. Wahab, M. S. Abdul Karim and M. S. Rahman, Design and optimization of π -shaped slotted dual-band SIW antenna for 5G applications, *Applications of Modelling and Simulation*, 9, 2025, 92–106.
- [4] J. Krupka, Microwave measurements of electromagnetic properties of materials, *Materials*, 14, 2021, 5097.
- [5] J. Sun, W. Wang and Q. Yue, Review on microwave-matter interaction fundamentals and efficient microwave-associated heating strategies, *Materials*, 9, 2016, 231.
- [6] N. S. I. Didik Aprianto, N. Hasan, N. I. I. Mohd Nadzri, N. Mustafa, L. F. Qi, A. A. Mohd Faudzi, N. A. Talip Yusof and M. S. Abdul Karim, Factorial analysis on the preparation of barium titanate-epoxy resin composite for antenna substrate, *Progress in Electromagnetics Research C*, 147, 2024, 127–134.
- [7] L. Liu, M. Ye and W. Xue, Silicon-on-insulator-based narrowband microwave photonic filter with widely tunable bandwidth, *Journal of Lightwave Technology*, 41, 2023, 6341–6347.
- [8] S. Stefanovski Pajovic, M. Potrebic and D. Tosic, Advanced filtering waveguide components for microwave systems, *Microwave Systems and Applications*, IntechOpen, 2017, 51–74.
- [9] N. S. Mat Hussain, A. N. Azman, N. A. Talip Yusof, N. A. A. Hj Mohtadzar and M. S. Abdul Karim, Design of resonator cavity for liquid material characterization, *TELKOMNIKA Telecommunication Computing Electronics and Control*, 20, 2022, 447–454.
- [10] M. Mrvic, S. Stefanovski Pajovic, M. Potrebic and D. Tosic, Design of microwave waveguide filters with effects of fabrication imperfections, *Facta Universitatis Series Electronics and Energetics*, 30, 2017, 431–458.
- [11] S. Sahin, N. K. Nahar and K. Sertel, A simplified Nicolson–Ross–Weir method for material characterization using single-port measurements, *IEEE Transactions on Terahertz Science and Technology*, 10, 2020, 404–410.
- [12] E. J. Rothwell, J. L. Frasch, S. M. Ellison, P. Chahal and R. O. Ouedraogo, Analysis of the Nicolson–Ross–Weir method for characterizing the electromagnetic properties of engineered materials, *Progress in Electromagnetics Research*, 157, 2016, 31–47.
- [13] J. Bonello, A. Demarco, I. Farhat, L. Farrugia and C. V. Sammut, Application of artificial neural networks for accurate determination of the complex permittivity of biological tissue, *Sensors*, 20, 2020, 4460.
- [14] Q. Tan, H. Zhu, W. Ma, Y. Yang and K. Huang, High temperature dielectric properties measurement system at 915 MHz based on deep learning, *International Journal of RF and Microwave Computer-Aided Engineering*, 29, 2019, e21948.
- [15] M. S. Sim, K. Y. You, R. Dewan, F. Esa, R. A. Rashid and K. Y. Lee, Advances in artificial neural network assisted microwave sensors for material characterization, *IEEE International Conference on Advanced Telecommunication and Networking Technologies*, 2024, 1–4.
- [16] G. C. Ram, S. Hanumantha Rao, G. R. L. V. N. Srinivasa Raju, D. Ramesh Varma, M. Venkata Subbarao, D. Girish Kumar, S. Tripura Siva Satya Tejaswini and P. Sai Naga Sreya, Design and development of a novel microwave sensor for biochemical detection, *Proceedings on Engineering Sciences*, 7, 2025, 1973–1980.

- [17] C. Gocen and M. Palandoken, UHF RFID microwave sensor tag design for an RSSI-based machine learning assisted binary ethanol–water mixture characterization, *IEEE Sensors Journal*, 24, 2024, 262–269.
- [18] M. S. Hossain, S. M. Iqbal and Y. Zhou, Microwave glucose concentration classification by machine learning, *IEEE Texas Symposium on Wireless and Microwave Circuits and Systems*, Waco, USA, 2020, 1–4.
- [19] M. Islam, C. L. Min, N. J. Shoumy, M. S. Ali, S. Khatun, M. S. Abdul Karim and B. S. Bari, Software module development for non-invasive blood glucose measurement using ultra-wideband and machine learning, *Journal of Physics Conference Series*, 1529, 2020, 052066.
- [20] H. Guo, L. Yao and F. Huang, A cylindrical cavity sensor for liquid water content measurement, *Sensors and Actuators A Physical*, 238, 2016, 133–139.
- [21] H. Kawabata, Y. Kobayashi and S. Kaneko, Analysis of cylindrical cavities to measure accurate relative permittivity and permeability of rod samples, *Asia-Pacific Microwave Conference*, Yokohama, Japan, 2010, 1459–1462.
- [22] S. Zinal and G. Boeck, Complex permittivity measurements using TE_{11p} modes in circular cylindrical cavities, *IEEE Transactions on Microwave Theory and Techniques*, 53, 2005, 1870–1874.
- [23] M. S. Bin Abdul Karim, N. Binti Abu Talip Yusof and T. Kitazawa, Scattering analysis of rectangular cavity with input and output waveguides and its application to material characterization, *IEEE Asia Pacific Microwave Conference*, Kuala Lumpur, Malaysia, 2017, 588–591.
- [24] W. Bacsá, R. Bacsá and T. Myers, Introduction: wave optics near surfaces, in *Wave Optics Near Surfaces*, 2020, 1–7.
- [25] T. Ozturk, M. Hudlička and Ī. Uluer, Development of measurement and extraction technique of complex permittivity using transmission parameter S₂₁ for millimeter wave frequencies, *Journal of Infrared Millimeter and Terahertz Waves*, 38, 2017, 1510–1520.
- [26] T. Han, Y. Seo and E. Choi, Significant reduction of resonant frequency by multi-layered dielectric material-loaded coaxial cavity for microwave heating, *Journal of Electromagnetic Engineering and Science*, 22, 2022, 1–7.
- [27] J. Baker-Jarvis, *Dielectric and Conductor-Loss Characterization and Measurements on Electronic Packaging Materials*, NIST Technical Note, Gaithersburg, USA, 2001.
- [28] A. Yakubu, Z. Abbas, N. Ibrahim and A. Fahad, The effect of ZnO nanoparticles filler on complex permittivity of ZnO–PCL nanocomposite at microwave frequency, *Physical Science International Journal*, 6, 2015, 196–202.
- [29] H. Ohsato, J. Varghese and H. Jantunen, Dielectric losses of microwave ceramics based on crystal structure, *Electromagnetic Materials and Devices*, IntechOpen, 2018.
- [30] I. R. Ibrahim, M. M. Rashid, M. R. Abdullah and M. A. Hassan, A study on microwave absorption properties of carbon black and Ni_{0.6}Zn_{0.4}Fe₂O₄ nanocomposites by tuning the matching-absorbing layer structures, *Scientific Reports*, 10, 2020, 3135.